

## Mechanical properties of individual focal adhesions probed with a magnetic microneedle

Benjamin D. Matthews,<sup>a,b</sup> Darryl R. Overby,<sup>a</sup> Francis J. Alenghat,<sup>a</sup> John Karavitis,<sup>a</sup> Yasuchi Numaguchi,<sup>a</sup> Philip G. Allen,<sup>c</sup> and Donald E. Ingber<sup>a,\*</sup>

<sup>a</sup> *Vascular Biology Program, Departments of Pathology and Surgery, Children's Hospital, Harvard Medical School, Boston, MA 02115, USA*

<sup>b</sup> *Department of Pediatrics, Massachusetts General Hospital, Harvard Medical School, Boston, MA 02115, USA*

<sup>c</sup> *Division of Hematology, Department of Medicine, Brigham and Women's Hospital, Harvard Medical School, Boston, MA 02115, USA*

### Abstract

A permanent magnetic microneedle was developed to apply tensional forces to integrin receptors via ligand-coated magnetic microbeads while optically analyzing the mechanical properties of individual focal adhesions. Force application (130 pN for 3 s) through activated  $\beta 1$  integrins produced less bead displacement than when unligated integrins were stressed. This strengthening response differed markedly on a bead-by-bead basis, correlated directly with local focal adhesion assembly, and was similar when analyzed at 4 °C, indicating that it was due to passive material properties of the cell. Viscoelastic analysis clarified that recruitment of focal adhesion proteins increased the local elastic stiffness of the adhesion complex without changing its viscous behavior. These data indicate that individual focal adhesions exhibit distinct mechanical properties that depend upon local focal adhesion assembly, and that these local variations in micromechanics can be detected and analyzed within living cells using the permanent magnetic microneedle technique.

© 2003 Elsevier Inc. All rights reserved.

*Keywords:* Mechanical stress; Integrins; Focal adhesion; Mechanotransduction; Cell mechanics; Magnetometry

The ability of cells to sense and respond to mechanical stresses that are transmitted between the intracellular environment and surrounding extracellular matrix (ECM) is critical for normal cellular behaviors, including motility, growth, and apoptosis [1–5]. When ECM is deformed, cells experience mechanical stress as a result of force transfer across transmembrane integrin receptors that mediate cell adhesion to ECM [6–8]. When cells move they transmit tractional forces from the internal cytoskeleton to the ECM over the same receptors [9,10]. The mechanical response of the cell to changes in the level of stress transmitted over integrins is governed predominantly by the internal cytoskeleton that mechanically couples to integrins within macromolecular adhesion complexes on the cell surface, known as focal adhesions [6,7,11]. Focal adhesion proteins, such as vinculin and paxillin that bind both integrins and actin filaments, form a molecular bridge that mediates force

transfer between integrins and the cytoskeleton in these regions [6,12,13]. Focal adhesions are also signaling complexes [7,8], and both their assembly and signaling activities change in response to applied stress [14–20]. However, very little is known about the mechanical properties of these critical adhesion structures, how one focal adhesion varies from another, or how their viscoelastic behavior is impacted by changes in their assembly.

Mechanical analyses of focal adhesions have been carried out using optical tweezers [17,18,21] and micro-magnetic [13,22–26] techniques. These studies revealed that, on average, force application to transmembrane integrins that form focal adhesions results in less membrane displacement (i.e., greater stiffness) than when the same stress is applied to other transmembrane receptors, or to integrins that fail to promote focal adhesion assembly [13,26–28]. However, most of the methods used in these studies estimated cellular mechanical properties based upon population averages obtained from many cells containing multiple focal adhesions per cell. This is

\* Corresponding author. Fax: 1-617-730-0230.

E-mail address: [donald.ingber@tch.harvard.edu](mailto:donald.ingber@tch.harvard.edu) (D.E. Ingber).

a complication because there is a high degree of variability in focal adhesion formation and micromechanical behavior, both between cells and at different locations in the same cell. The mechanical behavior of individual focal adhesions has been studied in the past [18–20,29], however, quantitative analysis of their viscoelastic properties was not carried out. Thus, it remains unclear how changes in adhesion complex structure and composition impact the local micromechanical response of the cell to mechanical stress.

In this study, we set out to characterize the mechanical properties of individual membrane adhesion complexes, and to directly determine the contribution of focal adhesion assembly to local changes in cell micromechanics. When cells bind to small (4.5  $\mu\text{m}$  diameter) microbeads coated with activating integrin ligands, they form well-developed focal adhesions containing both structural proteins (e.g., vinculin, paxillin, and F-actin) and various signaling molecules at the bead–membrane interface [15,30–33]. Use of similarly coated magnetic microbeads in conjunction with applied magnetic fields permits analysis of the response of individual focal adhesions to applied mechanical stress [13,22–25]. Here we describe a technique to analyze force–displacement relationships and viscoelastic properties of individual focal adhesions on the surfaces of living cells using a novel permanent magnetic microneedle, in conjunction with an automated micromanipulator and an optical microscope.

## Materials and methods

**Experimental system.** Bovine capillary endothelial cells (passage 10–15) were maintained at 37 °C in 10% CO<sub>2</sub> on tissue culture dishes in low glucose Dulbecco's modified Eagle's medium (DMEM; Gibco-

BRL) supplemented with 10% fetal calf serum (FCS) (Hyclone), 10 mM Hepes (JRH-Biosciences), and L-glutamine (0.292 mg/ml)/penicillin (100 U/ml)/streptomycin (100  $\mu\text{g}/\text{ml}$ ) (GPS) as previously described [1,34]. Cells were cultured in DMEM supplemented with low (0.5%) FCS for 24 h, trypsinized (Trypsin–EDTA, Gibco), collected, and then seeded ( $1.5 \times 10^4$  cells/dish) onto glass-bottomed 35 mm dishes (MatTek) that were pre-coated with 500 ng/cm<sup>2</sup> fibronectin. Cells were maintained in these dishes for 18–24 h prior to the experiment in serum-free DMEM with 10 mM Hepes, 0.5% bovine serum albumin (BSA), 10  $\mu\text{g}/\text{ml}$  human high density lipoprotein (Intracell), 5  $\mu\text{g}/\text{ml}$  holo-transferrin (Collaborative Research), and GPS.

Tosyl-activated super-paramagnetic beads (4.5  $\mu\text{m}$  diameter; Dynabeads M-450, Dynal) were coated with either synthetic RGD-containing peptide (peptide-2000, Integra) or non-integrin activating anti- $\beta 1$  antibody (K20, Immunogen) in pH 9.4 carbonate buffer as previously described [26,33]. Immediately before an experiment, cells were incubated with beads ( $\sim 20$  beads/cell) for 10 min and then washed multiple times with PBS to remove unbound beads prior to magnetic stress application. To maintain proper pH throughout the experiment, these studies were carried out in bicarbonate-free medium consisting of Hanks' Balanced Salts (Sigma), 10 mU/L MEM non-essential amino acids (Sigma), 20 ml/L MEM essential amino acids (Sigma), 2 mM L-glutamine (Sigma), 10 mM Hepes, pH 7.3, and 1% BSA.

**Permanent magnetic microneedle.** The magnetic microneedle system we developed to apply forces to magnetic beads consists of a stainless steel needle (48 mm long, 670  $\mu\text{m}$  shaft diameter, and 40  $\mu\text{m}$  tip diameter; Singer) attached to a permanent neodymium iron boron disc magnet (26 mm diameter, 6 mm height; Edmund Industrial Optics) (Fig. 1A). The magnet is attached to a 4 mm  $\times$  25 mm aluminum rod mounted on an electronic micromanipulator (Eppendorf). The force applied to each magnetic microbead is a function of the distance between the bead and the needle tip, and the mass magnetic susceptibility of the beads ( $16 \times 10^{-5}$  m<sup>3</sup>/kg for 4.5  $\mu\text{m}$  Dynal beads). Calibration of the forces generated by the magnetic needle was carried out by pulling the beads through glycerol solutions of known viscosity, as described previously [13].

**Magnetic pulling cytometry.** To measure the local mechanical properties of individual focal adhesions at bead-binding sites, cells with bound beads were maintained at 37 °C using a heated stage (Omega) and visualized on a Nikon Diaphot 300 microscope (Tokyo, Japan). The magnetic needle was then used to apply a 3 s force pulse

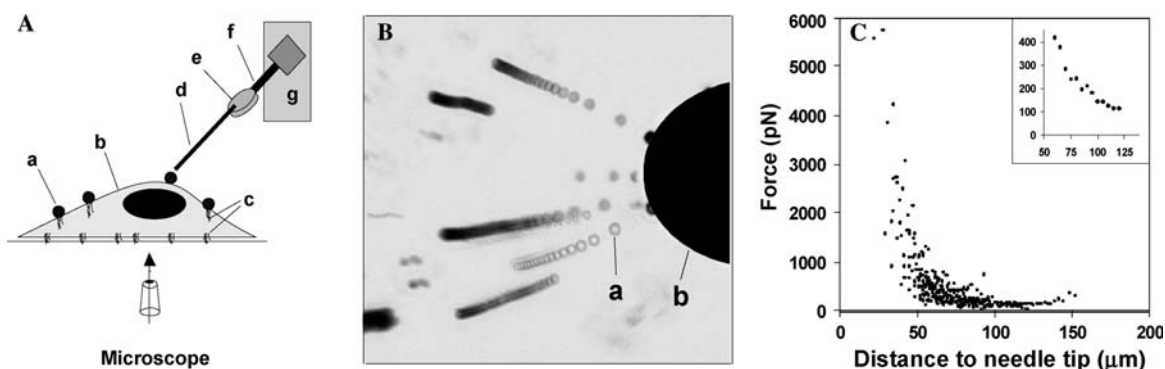


Fig. 1. The permanent magnetic microneedle device. (A) Magnetic microbeads coated with RGD-peptide or anti-integrin antibodies (a) that are added to the apical surface of cultured cells (b) induce local clustering of integrin receptors and associated recruitment of focal adhesion proteins (c). Force is applied to the cells via the attached microbeads using the magnet microneedle which consists of a stainless steel needle (d) attached to a permanent magnet (e) fastened to an aluminum rod (f) that is mounted on a micromanipulator (g) fastened to a microscope. (B) Composite of time-lapse images of bright field views showing magnetic microbeads being pulled through glycerol in response to magnetic stress application by the microneedle. The beads (a) are attracted to magnet along magnetic field lines perpendicular to the needle tip (b). (C) Force versus distance relationship for magnetic needle for 4.5  $\mu\text{m}$  diameter Dynal beads using the data generated in (B) from measurement of 20 beads at multiple positions. Inset shows the average force (pN) as a function of distance ( $\mu\text{m}$ ) between 50 and 125  $\mu\text{m}$  from the tip of the magnetic needle.

of 130 pN to the bead while bead displacement was measured optically. The manipulator speed was set to 1000  $\mu\text{m/s}$ , and the tip was oriented at  $45^\circ$  relative to the substrate and positioned within the culture medium 600  $\mu\text{m}$  away from the cell-bound beads to be tested. The needle tip was then rapidly brought within 70–100  $\mu\text{m}$  from the bead, held in position for 3 s and then quickly returned to its original position. Time lapse imaging (4 Hz) with a CCD camera (Hamamatsu, Japan) attached to the microscope was used to record bead motion. Image processing of frame sequences using IPLab (version 3.2.4, Scanalytics) was done to track the centroid position of each bead in time and to compute the maximum bead displacement in response to the applied force. All measurements were carried out within 60 min of bead binding. Multiple cells sampled from the same dish also were separated from each other by at least 2 mm to ensure against residual effects from previous force pulses. For real-time visualization of local focal adhesion assembly during force application, cells were transfected with plasmids encoding GFP–vinculin or paxillin using Effectene transfection reagent (Qiagen), or transduced with an adenoviral vector encoding EYFP–actin, as previously described [35].

To analyze the viscoelastic properties of individual focal adhesions, the bead displacement measured during the force pulse was fit to the 4-parameter viscoelastic creep model of Bausch et al. [22,23]. For these studies, a faster CCD camera (20 Hz; Roper Scientific) was used to improve temporal resolution of bead displacement. Nonlinear regression using least-squares minimization was performed using Mathematica (Wolfram Research) to compute the optimal parameter values for each of the two elastic and two viscous elements describing viscoelastic creep response for each bead.

## Results and discussion

To probe the mechanical properties of integrin–cytoskeleton linkages within individual focal adhesions, we fabricated a permanent magnetic microneedle to generate a high gradient magnetic field capable of applying tensional stresses to cells via adherent ligand-coated magnetic microbeads (Fig. 1). Calibration studies using the magnetic needle to pull 4.5  $\mu\text{m}$  magnetic beads through a high viscosity ( $\sim 1000$  centipoise) glycerol solution revealed that the beads experienced a force in the direction of the needle tip (Fig. 1B) that exceeded 5 nN in the immediate vicinity of the tip and decreased to approximately 130 pN when the beads were 100  $\mu\text{m}$  from the tip (Fig. 1C).

To analyze the mechanical properties of individual focal adhesions, adherent capillary endothelial cells were allowed to bind for 10 min to magnetic microbeads coated with a synthetic RGD-peptide that both binds and ligates (chemically activates) cell surface integrin receptors (Fig. 2A). The micromanipulator was then used to apply 130 pN force to each bead by rapidly moving the needle tip from a far distance to a point 100  $\mu\text{m}$  from a cell-bound bead; the needle tip was held in place for approximately 3 s, and then abruptly returned to its original distant position. Real-time optical microscopy was combined with computerized particle-tracking analysis to obtain sub-pixel resolution of bead displacement (Fig. 2B).

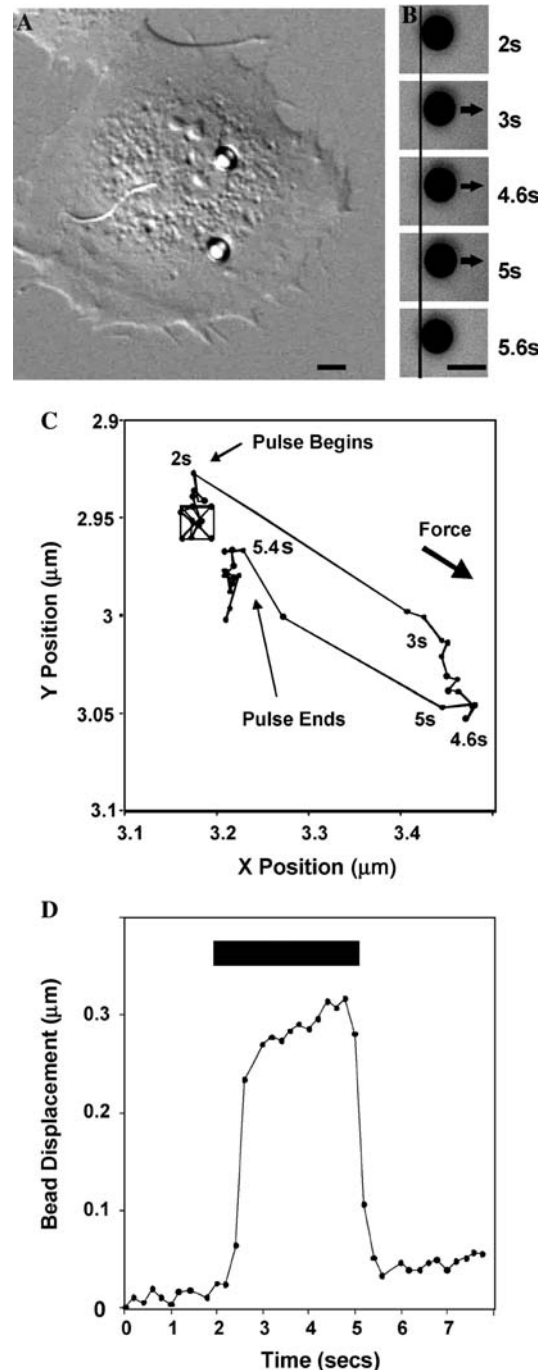


Fig. 2. Visualization and quantitation of microbead displacement on the surface membrane of cultured cells using computerized image processing. (A) A differential interference contrast view of an adherent cell with two 4.5  $\mu\text{m}$  RGD-beads bound to integrins on its apical surface. (B) A series of bright field images recorded over 8 s showing bead displacement to the right in response to application of a 3 s force (130 pN) pulse between 2 and 5 s of the recording period (arrows). (C) Map of changes in the X and Y positions of the bead shown in (B) during the same time course. Note the bead does not return to its original position after the force pulse ceases. (D) Bead displacement as a function of time before, during, and after the 3 s force pulse (solid rectangle). (Individual data points in (C) and (D) are 0.2 s apart; bars = 5  $\mu\text{m}$ ).

Application of 130 pN produced measurable changes in the position of RGD-beads that were bound to the cell-surface. Figs. 2C and D show the lateral motion of a bead that was displaced approximately 300 nm within the first second of the 3 s force pulse and then moved only minimally for the remainder of the pulse. Quantitation of displacement from multiple RGD-coated beads undergoing the same force regimen revealed a large variability in maximum displacement that ranged from less than 50 nm to over 1  $\mu\text{m}$  with a mean of  $95 \pm 56.7$  nm (SD). When the magnetic pulse ended, the beads recoiled by 70–95% within 0.5 s (Fig. 2D), and they typically did not return to their exact original position on the cell surface (Fig. 2C). Analysis of over 100 different RGD-beads on multiple cells revealed similar behavior.

To determine the influence of focal adhesion formation on the local mechanical properties of cell surface adhesion complexes, we compared the maximum displacement of beads coated with integrin-activating RGD peptide to beads coated with non-activating anti- $\beta 1$  integrin antibody (K20) following a 3 s force (130 pN) pulse. Binding of RGD-coated beads to the cell surface has been shown to activate integrin signaling and induce local focal adhesion assembly within minutes, whereas the non-activating K20-beads bind integrins to a similar extent without producing either effect [30,31,33]. Our studies revealed that the maximum displacement of RGD-beads was significantly less than the displacement observed for K20-beads ( $p < 0.01$  using ANOVA) (Fig. 3A). Importantly, when soluble RGD peptide was added to ligate and activate the K20-bound integrins, the maximum displacement was reduced to a level comparable to that exhibited by RGD-beads (Fig. 3A). These data indicate that clustering and activation of integrins significantly increase the stiffness of integrin–cytoskeleton linkages, possibly by promoting local focal adhesion assembly and transmission of mechanical stress to the internal cytoskeleton.

To further investigate the ability of RGD-coated beads to induce focal adhesion assembly and mechanical coupling to the cytoskeleton, we transfected endothelial cells with vectors encoding the focal adhesion proteins, vinculin, paxillin, or actin, linked to enhanced green or yellow fluorescent protein (EGFP or EYFP, respectively). We then applied a 3 s force (130 pN) pulse to RGD-beads that were bound to cells and analyzed the relationship between bead displacement and local fluorescence intensity. This is possible because, as previously demonstrated [30,31,33], not all surface-bound RGD-beads induce focal adhesion assembly. Importantly, RGD-beads that induced focal adhesion assembly, as indicated by recruitment of vinculin (Fig. 3B), actin or paxillin (not shown), were much stiffer than those that did not. Quantitation of results obtained with many beads confirmed that beads with vinculin or actin (Fig. 3C, left) exhibited a 5- to 8-fold reduction in maximum displacement, representing a local increase in focal adhesion stiffness ( $p$  always  $< 0.01$  using ANOVA). Moreover, similar results were obtained when the effects of GFP–paxillin recruitment were analyzed (not shown). These data indicate that individual focal adhesions within a single cell exhibit distinct mechanical properties that strongly depend upon local recruitment of focal adhesion and cytoskeletal proteins, despite local integrin binding to RGD.

Maturation and strengthening of existing focal adhesions occurs following application of external mechanical force to integrins [14–20]. Therefore, the observed differences in bead displacement during the 3 s force pulse could potentially arise from mechanical induction of active biochemical remodeling events within the local focal adhesion. To distinguish such an active process from the intrinsic passive material properties of the focal adhesion, similar force–displacement studies were performed in cells that were chilled to 4  $^{\circ}\text{C}$  after binding to RGD-coated beads so as to suppress

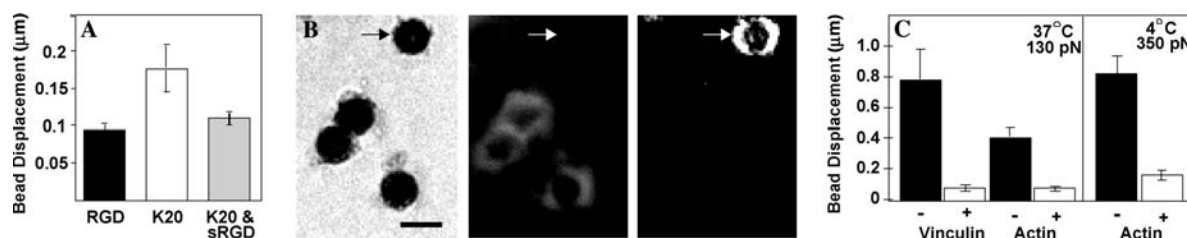


Fig. 3. Integrin activation and focal adhesion formation influence the mechanics of individual bead complexes. (A) A 3 s force (130 pN) pulse induced less bead displacement when applied to activating RGD-beads compared to non-activating K20-beads. Addition of soluble RGD (sRGD) peptide to ligate and activate the K20-bound integrins promoted strengthening of these bead attachments. (B) A cell transfected with GFP–vinculin and bound to 4 RGD-beads viewed by bright field (left) or fluorescence (middle) microscopy showing that vinculin was only recruited to 3 of the 4 bound beads (arrow indicates a bound bead that did not exhibit vinculin staining). When bright field images recorded before and after application of a 3 s force (130 pN) pulse were digitally subtracted (right), only the bead that failed to recruit vinculin exhibited significant bead displacement (white crescent, arrow). (C) Bound RGD-beads that recruited vinculin and actin (+) exhibited less displacement in response to application of a 3 s force (130 pN) pulse than those that did not (–) (left). Similar results were noted when a larger force (350 pN) was applied at 4  $^{\circ}\text{C}$  (right). Bar = 5  $\mu\text{m}$ .

biochemical remodeling during the 3 s of force application. For these studies, a larger force of 350 pN was used, because the 130 pN force produced negligible bead displacement at this reduced temperature. However, with this greater force, a significantly lower displacement could again be detected for RGD-beads that recruited EYFP-actin than those that did not, despite being at 4 °C (Fig. 3E, right,  $p < 0.01$  using ANOVA). These results suggest that the force–displacement relationships indeed arise from the intrinsic passive material properties of individual focal adhesions, as opposed to an active strengthening mechanism, at least over the brief (3 s) period we analyzed.

Focal adhesion proteins, such as vinculin and actin, are known to influence local cellular stiffness and focal adhesion strength [12,13,26], yet it is not well understood how heterogeneity in focal adhesion composition influences local mechanical behavior. We therefore chose to analyze the viscoelastic properties of individual focal adhesions, and to relate those properties to focal adhesion assembly, as indicated by recruitment of EYFP-actin to the bead complex. The viscoelastic analysis was performed by first measuring the displacement of an RGD-bead in response to a 3 s force pulse and then fitting this displacement ( $d$ ) to the viscoelastic creep model of Bausch et al. [22,23]:

$$d(t) = \frac{F}{k_0} \left( 1 - \frac{k_1}{k_0 + k_1} \exp(-t/\tau) \right) + \frac{F}{\gamma_0} t, \quad (1a)$$

where

$$\tau = \frac{\gamma_1(k_0 + k_1)}{k_0 k_1}. \quad (1b)$$

Here,  $F$  is the applied force (130 pN),  $t$  is time, and  $k_0$ ,  $k_1$ ,  $\gamma_0$ , and  $\gamma_1$  are the fitted parameters describing the two elastic and two viscous elements of the viscoelastic body shown in Fig. 4A;  $\tau$  is the time constant describing the transition from elastic to viscous behavior [22,23]. Representative displacements for two RGD-beads bound to the same cell with and

without EYFP-actin recruitment are shown in Fig. 4B, along with the optimized least-squares fits from Eq. (1). The viscoelastic creep response is characterized by an immediate elastic displacement described by  $F/(k_0 + k_1)$ , followed by a transition to viscous-dominated behavior where displacement increases linearly with time with slope  $F/\gamma_0$ . Analysis of the fitted viscoelastic parameters for multiple beads revealed a 4-fold reduction in total elastic compliance  $1/(k_0 + k_1)$  for focal adhesions that recruited EYFP-actin compared to those that did not ( $p < 10^{-5}$ ,  $N = 52$ ), while late-time viscous behavior, as described by  $1/\gamma_0$ , and the viscoelastic time constant  $\tau$  remained relatively unchanged ( $p = 0.23$ ,  $p = 0.66$ ) (Figs. 4C–E). These data indicate that differential recruitment of focal adhesion proteins strongly influences the micromechanical properties of these cell adhesion sites primarily by changing the elastic stiffness, without significantly affecting their viscous behavior.

Previous studies of cellular biomechanics have typically involved population-based averages over many focal adhesions using ligand-coated magnetic particles [13,22,23,25,26,28,36], where the influence of mechanical heterogeneity for local variations in cell mechanics has not been considered. In the few studies where the structure and properties of individual focal adhesions have been probed (e.g., using optical tweezers, micropipettes, and microfabricated substrates; [18–21,29]), micromechanical and viscoelastic properties have not been quantitated. In light of our current findings, population-based reports of cell and focal adhesion mechanics are likely biased towards the decreased elastic stiffness of those focal adhesions that fail to form mechanical coupling with the internal cytoskeleton. Instead, our studies suggest that the micromechanical properties of cells and focal adhesions can be more appropriately assessed by relating the measured mechanical properties to local changes in focal adhesion assembly.

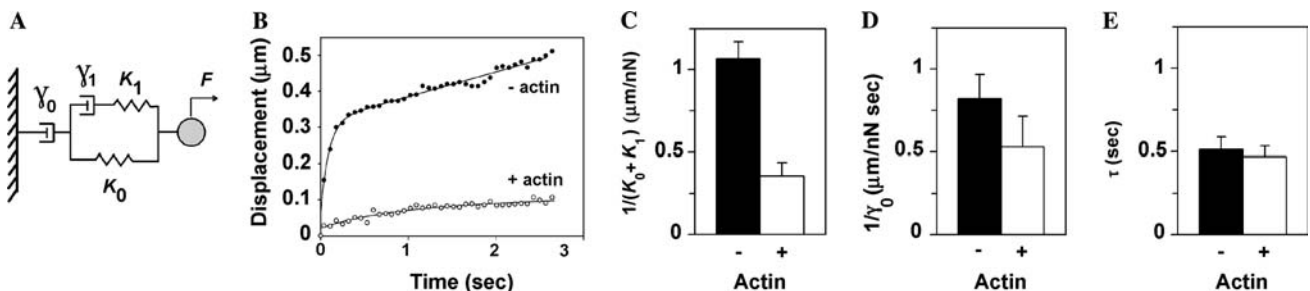


Fig. 4. Viscoelastic analysis of individual focal adhesions induced by binding of RGD-beads. (A) The viscoelastic model of Bausch et al. [22,23] consisting of 2 elastic ( $k_0$ ,  $k_1$ ) and 2 viscous ( $\gamma_0$ ,  $\gamma_1$ ) elements to produce the creep response shown in Eq. (1). (B) Representative creep responses measured from 2 beads on the same cell that did (open circles) or did not (filled circles) exhibit EYFP-actin recruitment. Curves represent the optimized fits to the viscoelastic creep model (Eq. (1)). (C–E) Average total elastic compliance  $1/(k_0 + k_1)$  (C), late viscous slope ( $1/\gamma_0$ ) (D), and viscoelastic time constant ( $\tau$ ) (E) measured within individual adhesion complexes associated with RGD-beads with (+) or without (-) EYFP-actin staining.

In summary, our findings show that the permanent magnetic needle provides a direct means to analyze the mechanical properties of individual adhesion complexes on the cell surface, and in conjunction with fluorescence and optical microscopy, to relate these micro-mechanical properties to local subcellular architecture. Because the permanent magnetic needle can provide a reproducible force and is harmless to the cell at the levels of force used here, this simple device provides an attractive system with which to study the mechanical properties of individual focal adhesions. Using this system, we showed that focal adhesion reinforcement of integrin–cytoskeleton linkages locally increases the mechanical stiffness of this adhesion complex by reducing its elasticity, without altering its viscous properties. Our findings also emphasize the need to combine biophysical measurements of cell mechanics with optical methods that permit simultaneous identification of changes in molecular remodeling at the site of force application.

### Acknowledgment

This work was supported by a grant from the Department of Defense (N00014-01-1-0782).

### References

- [1] C.S. Chen, M. Mrksich, S. Huang, G.M. Whitesides, D.E. Ingber, Geometric control of cell life and death, *Science* 276 (1997) 1425–1428.
- [2] J. Folkman, A. Moscona, Role of cell shape in growth control, *Nature* 273 (1978) 345–349.
- [3] D.E. Ingber, Fibronectin controls capillary endothelial cell growth by modulating cell shape, *Proc. Natl. Acad. Sci. USA* 87 (1990) 3579–3583.
- [4] R. Singhvi, A. Kumar, G.P. Lopez, G.N. Stephanopoulos, D.I. Wang, G.M. Whitesides, D.E. Ingber, Engineering cell shape and function, *Science* 264 (1994) 696–698.
- [5] C.J. Meyer, F.J. Alenghat, P. Rim, J.H. Fong, B. Fabry, D.E. Ingber, Mechanical control of cyclic AMP signalling and gene transcription through integrins, *Nat. Cell Biol.* 2 (2000) 666–668.
- [6] K. Burridge, M. Chrzanowska-Wodnicka, Focal adhesions, contractility, and signaling, *Annu. Rev. Cell. Dev. Biol.* 12 (1996) 463–518.
- [7] B. Geiger, A. Bershadsky, R. Pankov, K.M. Yamada, Transmembrane crosstalk between the extracellular matrix–cytoskeleton crosstalk, *Nat. Rev. Mol. Cell Biol.* 2 (2001) 793–805.
- [8] B. Geiger, A. Bershadsky, Assembly and mechanosensory function of focal contacts, *Curr. Opin. Cell Biol.* 13 (2001) 584–592.
- [9] M.P. Sheetz, D.P. Felsenfeld, C.G. Galbraith, Cell migration: regulation of force on extracellular-matrix–integrin complexes, *Trends Cell Biol.* 8 (1998) 51–54.
- [10] M. Dembo, Y.L. Wang, Stresses at the cell-to-substrate interface during locomotion of fibroblasts, *Biophys. J.* 76 (1999) 2307–2316.
- [11] D.R. Critchley, Focal adhesions—the cytoskeletal connection, *Curr. Opin. Cell Biol.* 12 (2000) 133–139.
- [12] R.M. Ezzell, W.H. Goldmann, N. Wang, N. Parasharama, D.E. Ingber, Vinculin promotes cell spreading by mechanically coupling integrins to the cytoskeleton, *Exp. Cell Res.* 231 (1997) 14–26.
- [13] F.J. Alenghat, B. Fabry, K.Y. Tsai, W.H. Goldmann, D.E. Ingber, Analysis of cell mechanics in single vinculin-deficient cells using a magnetic tweezer, *Biochem. Biophys. Res. Commun.* 277 (2000) 93–99.
- [14] J. Chen, B. Fabry, E.L. Schiffrin, N. Wang, Twisting integrin receptors increases endothelin-1 gene expression in endothelial cells, *Am. J. Physiol. Cell Physiol.* 280 (2001) C1475–C1484.
- [15] M.E. Chicurel, R.H. Singer, C.J. Meyer, D.E. Ingber, Integrin binding and mechanical tension induce movement of mRNA and ribosomes to focal adhesions, *Nature* 392 (1998) 730–733.
- [16] M. Chrzanowska-Wodnicka, K. Burridge, Rho-stimulated contractility drives the formation of stress fibers and focal adhesions, *J. Cell Biol.* 133 (1996) 1403–1415.
- [17] D.P. Felsenfeld, P.L. Schwartzberg, A. Venegas, R. Tse, M.P. Sheetz, Selective regulation of integrin–cytoskeleton interactions by the tyrosine kinase Src, *Nat. Cell Biol.* 1 (1999) 200–206.
- [18] C.G. Galbraith, K.M. Yamada, M.P. Sheetz, The relationship between force and focal complex development, *J. Cell Biol.* 159 (2002) 695–705.
- [19] D. Rivelino, E. Zamir, N.Q. Balaban, U.S. Schwarz, T. Ishizaki, S. Narumiya, Z. Kam, B. Geiger, A.D. Bershadsky, Focal contacts as mechanosensors: externally applied local mechanical force induces growth of focal contacts by an mDia1-dependent and ROCK-independent mechanism, *J. Cell Biol.* 153 (2001) 1175–1186.
- [20] N.Q. Balaban, U.S. Schwarz, D. Rivelino, P. Goichberg, G. Tzur, I. Sabanay, D. Mahalu, S. Safran, A. Bershadsky, L. Addadi, B. Geiger, Force and focal adhesion assembly: a close relationship studied using elastic micropatterned substrates, *Nat. Cell Biol.* 3 (2001) 466–472.
- [21] D. Choquet, D.P. Felsenfeld, M.P. Sheetz, Extracellular matrix rigidity causes strengthening of integrin–cytoskeleton linkages, *Cell* 88 (1997) 39–48.
- [22] A.R. Bausch, F. Ziemann, A.A. Boulbitch, K. Jacobson, E. Sackmann, Local measurements of viscoelastic parameters of adherent cell surfaces by magnetic bead microrheometry, *Biophys. J.* 75 (1998) 2038–2049.
- [23] A.R. Bausch, W. Moller, E. Sackmann, Measurement of local viscoelasticity and forces in living cells by magnetic tweezers, *Biophys. J.* 76 (1999) 573–579.
- [24] A.R. Bausch, U. HELLERER, M. Essler, M. Aepfelbacher, E. Sackmann, Rapid stiffening of integrin receptor–actin linkages in endothelial cells stimulated with thrombin: a magnetic bead microrheology study, *Biophys. J.* 80 (2001) 2649–2657.
- [25] B. Fabry, G.N. Maksym, J.P. Butler, M. Glogauer, D. Navajas, J.J. Fredberg, Scaling the microrheology of living cells, *Phys. Rev. Lett.* 87 (2001) 148102.
- [26] N. Wang, J.P. Butler, D.E. Ingber, Mechanotransduction across the cell surface and through the cytoskeleton, *Science* 260 (1993) 1124–1127.
- [27] H. Huang, R.D. Kamm, P.T. So, R.T. Lee, Receptor-based differences in human aortic smooth muscle cell membrane stiffness, *Hypertension* 38 (2001) 1158–1161.
- [28] N. Wang, D.E. Ingber, Probing transmembrane mechanical coupling and cytomechanics using magnetic twisting cytometry, *Biochem. Cell Biol.* 73 (1995) 327–335.
- [29] J.L. Tan, J. Tien, D.M. Pirone, D.S. Gray, K. Bhadriraju, C.S. Chen, Cells lying on a bed of microneedles: an approach to isolate mechanical force, *Proc. Natl. Acad. Sci.* (2003) (in press).

- [30] S. Miyamoto, S.K. Akiyama, K.M. Yamada, Synergistic roles for receptor occupancy and aggregation in integrin transmembrane function, *Science* 267 (1995) 883–885.
- [31] S. Miyamoto, H. Teramoto, O.A. Coso, J.S. Gutkind, P.D. Burbelo, S.K. Akiyama, K.M. Yamada, Integrin function: molecular hierarchies of cytoskeletal and signaling molecules, *J. Cell Biol.* 131 (1995) 791–805.
- [32] G.E. Plopper, H.P. McNamee, L.E. Dike, K. Bojanowski, D.E. Ingber, Convergence of integrin and growth factor receptor signaling pathways within the focal adhesion complex, *Mol. Biol. Cell* 6 (1995) 1349–1365.
- [33] G. Plopper, D.E. Ingber, Rapid induction and isolation of focal adhesion complexes, *Biochem. Biophys. Res. Commun.* 193 (1993) 571–578.
- [34] J. Yu, A. Moon, H.R. Kim, Both platelet-derived growth factor receptor (PDGFR)-alpha and PDGFR-beta promote murine fibroblast cell migration, *Biochem. Biophys. Res. Commun.* 282 (2001) 697–700.
- [35] S. Hu, J. Chen, B. Fabry, Y. Numaguchi, A. Gouldstone, D.E. Ingber, J.J. Fredberg, J.P. Butler, N. Wang, Intracellular stress tomography reveals stress focusing and structural anisotropy in cytoskeleton of living cells, *Am. J. Physiol. Cell Physiol.* 285 (2003) C1082–1090.
- [36] G.N. Maksym, B. Fabry, J.P.D. Navajas, D.J. Tschumperlin, J.D. Laporte, J.J. Fredberg, Mechanical properties of cultured airway smooth muscle cells from 0.05 to 0.4 Hz, *J. Appl. Physiol.* 89 (2000) 1619–1632.